Journal of Science and Transport Technology
Journal homepage: https://jstt.vn/index.php/en

An application of the response surface method to structural optimization problems

Anh Tuan Tran[1], Nhu Son Doan[2,*]
[1]University of Transport Technology, 54 Trieu Khuc, Thanh Xuan, Hanoi 100000, Vietnam
[2]Faculty of Civil Engineering, Vietnam Maritime University, 484 Lach Tray Street, Le Chan district, Haiphong 180000, Vietnam

Article info
Type of article:
Original research paper

DOI:
https://doi.org/10.58845/jstt.utt.2025.en.5.2.19-30

***Corresponding author:**
Email address:
vanson.ctt@vimaru.edu.vn

Received: 15/02/2025
Received in Revised Form: 12/04/2025
Accepted: 15/04/2025

Abstract: Structural problems are commonly analyzed using implicit solvers, such as the finite element method (FEM), which often demand manual processes and are computationally intensive, especially for structural optimization problems that involve multiple FEM evaluations to identify the optimal design solutions. In addition, implementing optimization algorithms also demands significant expertise for accurate application. This study proposes a simple yet efficient procedure to address structural optimization problems by transforming the implicit analysis into explicit performance functions using the response surface method and simulating the space of input variables by random samples. The explicit performance functions enable quick evaluations for all generated samples of inputs, and a search routine is developed to identify optimal solutions efficiently. The proposed procedure is validated through three case studies, demonstrating its ability to achieve accurate solutions within minutes of analysis.

Keywords: Response surface method; Structural optimization; Random simulations.

1. Introduction

Most structural problems are now solved using finite element methods, thanks to the rapid development of computer technology [1]. Many commercial software packages are available for structural analysis [2,3]. For example, SAP2000 and ETABS are commonly used for building structures, while MIDAS Civil or RM Bridge are widely applied to bridge structures. These fundamental software tools support various types of analysis, such as static, dynamic, transient, linear, and nonlinear analyses [4].

Recently, more advanced software such as ANSYS, ADINA, or ABAQUS has been introduced to handle more complex analyses [5]. With enhanced element types, boundary conditions (e.g., contacts, interactions), material models, and advanced analysis methods, these tools are well-suited for tackling complex engineering problems [6]. However, these advanced software packages are often expensive [7]. Additionally, computational time increases significantly for more complex analyses. For instance, solving time-history or nonlinear analyses may take hours of computation [4,8].

Furthermore, many problems require repetitive analyses, such as optimization or reliability assessments [9,10]. For these types of problems, computing time can escalate to days or even weeks [11]. To address this challenge, various

approximation methods have been proposed to accelerate the analyses. Response surface methods and machine learning-based surrogate models have gained prominence in tackling these problems [12–14]. While machine learning techniques are powerful, they require sufficient expertise to ensure appropriate hyperparameter selection and result interpretation [7]. Alternatively, response surface methods (RSM) are widely applied to engineering problems [13,15–17]. The core concept of RSM involves first establishing a set of input variable samples, commonly referred to as design of experiments (DOEs), and then obtaining true responses using actual models. Subsequently, mathematical equations, known as the response surface functions (RSFs), are developed to best fit the initial experimental data [18]. The RSFs then serve as surrogate models, replacing the original computationally expensive problems. By leveraging the RSF, the computational effort required for the initial problems can be significantly reduced.

Optimization is a crucial task in the design process, as it helps minimize investment costs while ensuring compliance with technical requirements [19]. For instance, multiple design solutions may satisfy a given load-carrying requirement, but their associated costs can vary significantly. Therefore, selecting the most cost-effective solution is essential to balancing technical performance and economic feasibility. However, optimizations often demand extensive computations due to their iterative nature, demanding significant computing time and effort, especially for implicit problems such as structural optimizations [19,20]. For example, optimizing the cost of a three-story frame requires at least 20 iterations, each involving a finite element method (FEM)-based analysis to achieve the optimal design [20].

Considering the aforementioned drawbacks, this study introduces a practical and effective method for addressing structural optimization problems. The proposed approach consists of two main steps. First, the implicit nature of structural analyses, which typically depend on complex numerical solvers such as FEM, is reformulated into explicit performance functions. This transformation is achieved using the RSM, which simplifies the structural behavior into more manageable mathematical models. Second, random simulations are conducted to generate diverse sets of input variables, thereby covering a broad range of potential design scenarios. The explicit formulation of the performance functions significantly accelerates their evaluation compared to traditional FEM computations. Furthermore, a tailored search routine is developed to systematically explore the generated input sets and identify optimal design solutions.

The remainder of this study is organized as follows. Section 2 details the procedure for constructing RSFs and describes a routine that integrates RSFs with random simulations for optimization. Section 3 presents numerical examples to evaluate the efficiency and accuracy of the proposed approach. Section 4 provides important discussions, and Section 5 concludes the study.

2. Methods

2.1. A brief summary of RSM

The response surface method is a well-established approximation technique for modeling computationally expensive processes. It begins with a well-designed experiment, where a set of input samples is generated, and their corresponding responses are determined using the original problem. Subsequently, explicit mathematical functions are formulated to best fit the experimental data. These functions, commonly referred to as empirical models or RSFs, provide an efficient approximation of the underlying problem. The main steps for implementing RSM are outlined below, while further details can be found in the literature, e.g., [17,18,21].

Step 1: Generate a set of input variables. This step, commonly referred to as the design of experiments, involves selecting an appropriate

sampling strategy. Box-Behnken design (BBD) and central composite design (CCD) are widely used in practice. Notably, for high-dimensional problems, CCD-based DOE results in a significantly larger sample size compared to BBD, making BBD a more practical choice in certain cases.

Step 2: Obtain responses for the DOE of the input set. The true experiments or actual problem evaluations are performed for each sample in the input set generated in Step 1.

Step 3: Construct response functions. Exponential and polynomial functions are commonly used to approximate the system's behavior. In general, quadratic polynomials are suitable for most engineering applications [10,22,23], and they are adopted in this work.

2.2. Random simulation for optimization problems

In optimization problems, a feasible domain of input variables is typically defined first. The optimal solution is then sought within this domain. Generally, optimization methods can be broadly classified into gradient-based (deterministic) methods and stochastic (metaheuristic) methods [9]. The former is applicable when the objective function is explicitly defined, whereas the latter is more robust as it can handle both explicit and implicit problems.

Considering a simple example of an optimization problem, as shown in Eq. (1):

$$\min_{x} f(x) = -\frac{1}{2}x^3 + 3x^2 - 2 \quad \text{s.t.} \quad -2 \le x \le 5 \tag{1}$$

It is well known that the optimal solution for this explicit objective function can be obtained using a gradient-based method. This involves first finding the critical points by setting the derivative of f(x) to zero and then evaluating the objective function at these points. To determine the global minimum, the function values at the critical points are compared with those at the domain boundaries.

Alternatively, stochastic methods can also be used to search for the optimal solution. The problem can be solved numerically by evaluating the objective function at a large random set of *x* values within its domain. Fig. 1 shows the results of 1,000 evaluations corresponding to 1,000 randomly generated samples of *x* in the range [−2, 5]. Since the objective function is evaluated numerically for these samples, the minimum value can be easily identified among the 1,000 computed values, as indicated by the star marker in Fig. 1. This approach is commonly known as Monte Carlo simulation-based optimization.

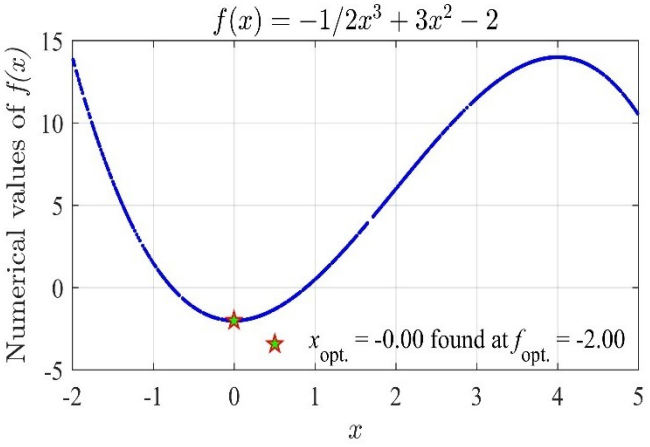

Fig. 1. An illustration of the stochastic optimization

Unlike gradient-based methods, which require explicit derivatives, stochastic methods provide a simple yet flexible way to estimate the optimal solution, particularly when the objective function is complex or non-differentiable. Clearly, the stochastic approach eliminates the need for derivative calculations but requires a large number of function evaluations. However, computing objective values can become challenging when the function is implicitly defined or costly to evaluate experimentally. Conversely, for explicitly defined objective functions and constraints, numerical evaluations remain feasible and convenient. Hence, integrating the stochastic approach with the RSM offers a practical and effective strategy for structural optimizations.

The stochastic approach described above can be extended to optimization problems with multiple variables and constraints, as outlined below. Notably, the RSM introduced in Subsection 2.1 will be utilized in Step 3 to develop explicit

models for constraint requirements.

Step 1: Randomly generate a large sample set for all input variables.

Step 2: Compute objective function values for the samples created in Step 1.

Step 3: Evaluate constraint conditions to identify feasible samples within the suitable domain.

Step 4: Determine the optimal objective value from the computed results in Steps 2 and 3.

Step 5: Identify the optimal variables by matching them to the optimal objective value obtained in Step 4.

3. Illustrative examples

In this section, three structural optimization problems are examined. The first example investigates the stochastic optimization presented in Subsection 2.2 for explicit constraints. The last two examples handle implicit constraints, where the response surface method and stochastic optimization outlined in Section 2 are combined to search for optimal solutions.

3.1. Example 1

This example is adapted from the previous work [24]. A cantilever beam subjected to a concentrated load Q, as shown in Fig. 2, is designed to satisfy both strength and serviceability requirements, as defined in Eq. (2). In Eq. (2), constraints for limiting deformation and stress are given in Eq. (2a) and (2b), respectively. Here, y_{LS} represents the maximum allowable deformation, while $[\sigma]$ denotes the material strength. In this example, y_{LS} is set to 1 cm, and $[\sigma]$ is 120 MPa. The optimization problem aims to minimize the beam's weight by selecting the optimal width and height of its cross-section. The initial parameters for this example are summarized in Table 1.

$$\frac{4QL^3}{Ebh^3} \le y_{LS} \quad (2a)$$

$$\frac{6QL}{bh^2} \le [\sigma] \quad (2b)$$

Mathematically, the problem can be written in Eq. 3. In Eq. (3), V denotes the volume of the beam, while FS_{Ser} and FS_{Str} represent the safety factors corresponding to the serviceability and the strength conditions.

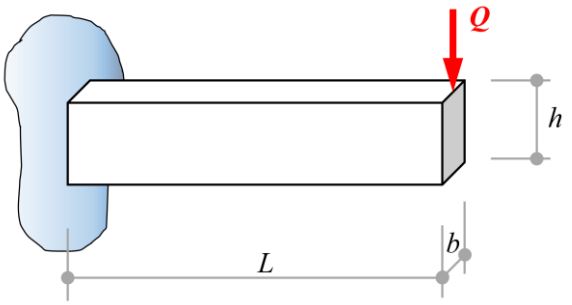

Fig. 2. The problem of a cantilever beam

Table 1. Considered uncertainties

Symbol	Description	Value	Unit
Q	Load	400	kN
E	Young's modulus	200	GPa
L	Beam length	2	m
b	Section width	4-36	cm
h	Section height	8-72	cm
$[\sigma]$	Strength limit	120	MPa
y_{LS}	Limit of deformation	1	cm

$$\begin{aligned} V_{Opt} &= \min V = \arg\min_{b,h}(Lbh) \\ \text{s.t.} \quad & FS_{Ser} \ge 1 \\ & FS_{Str} \ge 1 \end{aligned} \quad (3)$$

Since the problem is explicitly defined, the analytical solution can be easily obtained, as shown in Fig. 3—Fig. 3(a) for the serviceability constraint and Fig. 3(b) for the strength condition. In the figures, the dark regions indicate infeasible zones, while the white areas represent safety zones. The dot red lines depict the contours of the beam volumes. The results indicate a positive correlation between beam volume and the width and height of the section. The optimal dimensions of 0.08 m for the width and 0.72 m for the height are identified, as indicated by the star markers in the two figures.

Using the proposed method in Subsection 2.2, numerical solutions are presented in Figs. 4 and 5. In Fig. 4, the search domain is represented by 100,000 input samples uniformly distributed within their space. Based on these samples, the strength and serviceability requirements, as well as

the objective function, are evaluated and presented in Fig. 5. The horizontal axes in Fig. 5 represent safety factors, while the vertical axes correspond to beam volume.

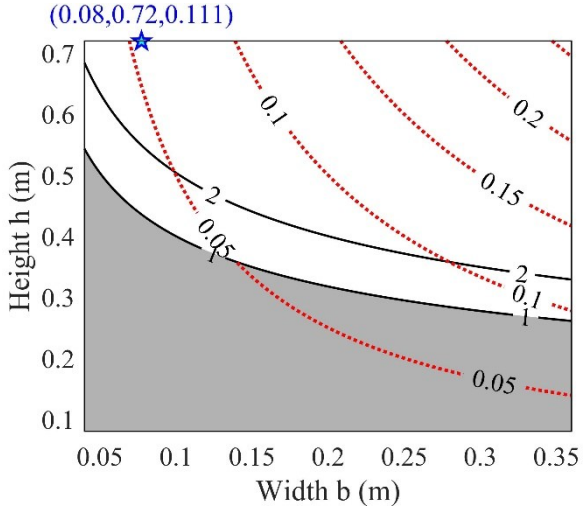

(a)

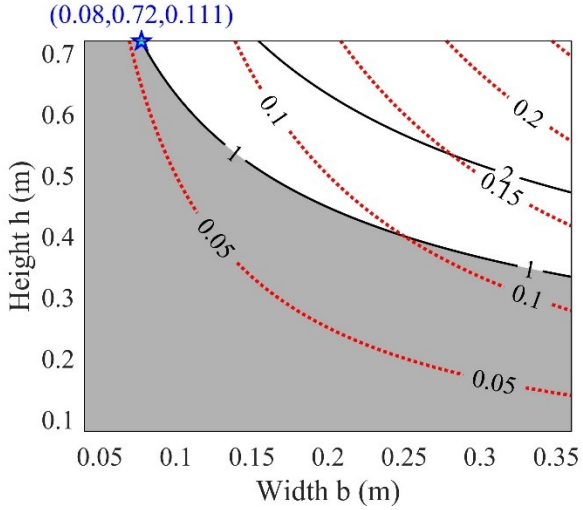

(b)

Fig. 3. Analytical solutions for Example 1: (a) contours of strength requirement and volume; (b) contours of serviceability requirement and volume

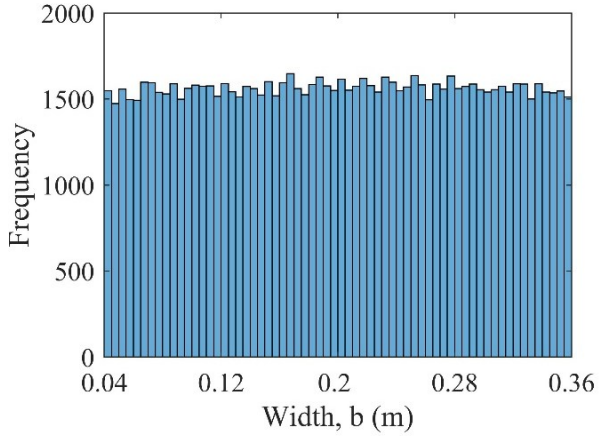

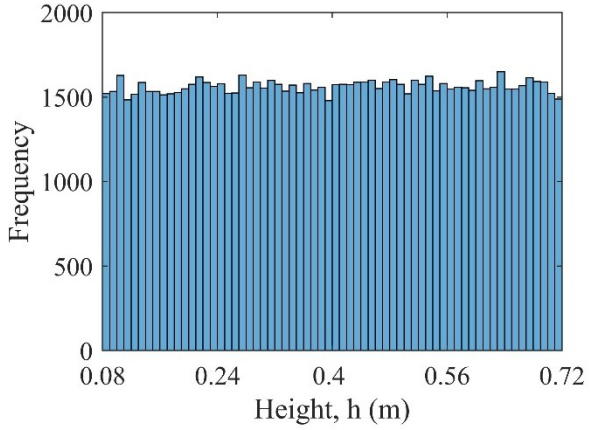

Fig. 4. Random simulations of inputs for Example 1

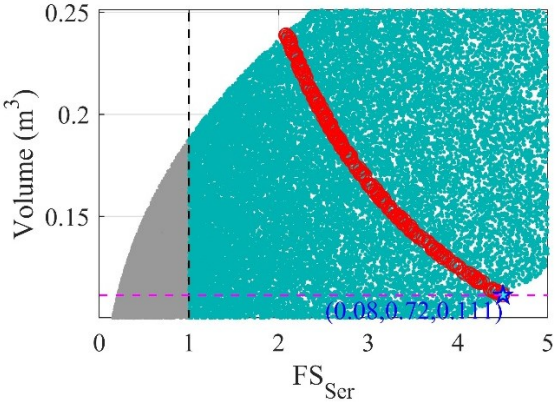

(a)

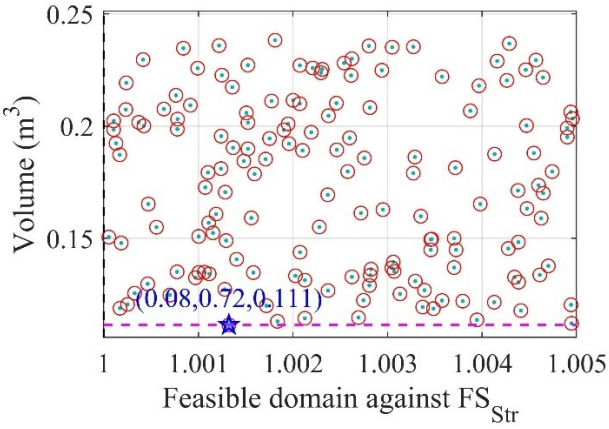

(b)

Fig. 5. Results obtained by the proposed procedure for Example 1: (a) Volumes estimated for all samples; (b) Optimal volume

In Fig. 5(a), dark points indicate infeasible samples that violate the serviceability condition ($FS_{Ser} < 1$), whereas green points denote feasible samples satisfying $FS_{Ser} \geq 1$. The search routine is applied to identify feasible solutions – those satisfying both design conditions and providing minimum volume – as highlighted by red markers in the figures. Notably, the limit values (FS equal to

unity) are indicated by the vertical dashed lines in the figure. Fig. 5(b) further refines the results by displaying samples closest to the strength limit state (i.e., FS_{Str} closest to unity). Ultimately, the optimal solution is identified, marked by star symbols in the figure. It is observed that the optimal solution (i.e., the minimum volume of 0.111 m^3 denoted by the star marker in Fig. 5) exactly matches the analytical result in Fig. 3, which demonstrates the accuracy of the proposed procedure.

3.2. Example 2

In Example 1, the objective functions and constraint equations are explicitly defined, allowing for fast and convenient computations across a large set of input samples. In this subsection, a two-story frame, shown in Fig. 6, is examined. The frame has a height of 6 m and a span of 5 m. The columns and beams have rectangular cross-sections, with widths and heights of 0.2 m × 0.2 m and 0.2 m × 0.3 m, respectively. The frame is made of concrete with an elastic modulus of 30 GPa and subjected to a uniformly distributed load of q = 5 kN/m acting on the left columns, as illustrated in Fig. 6. The optimization problem is to determine the optimal widths of the beams (b_b) and columns (b_c) that minimize the frame's weight. The widths are assumed to be in the range from 12 cm to 28 cm. A maximum top-story drift of 1.5 cm is imposed as a constraint for the drift of the frame (x).

Using uniform distributions, input samples are generated within their domains, as shown in Fig. 7. It is observed that the samples are distributed within the range of 12 cm to 28 cm. The RSM is then applied to construct the RSF for approximating the drift behaviors. Using the CCD, the sample set and corresponding drift values are summarized in Table 2. Notably, nine samples are generated for the two design variables, as shown in the table. The drifts (x) of the frame are analyzed for each sample, and the safety factors (defined by FS = 1.5/x) are summarized in the final column of Table 2. Based on these data, a full quadratic polynomial to estimate FS for any new input is easily established, as shown in Eq. (4). Fig. 8 compares the safety factors predicted by Eq. (4) with true values obtained directly from the FEM for 100 random samples. The results indicate that the RSF provides highly accurate approximations, as demonstrated by a high coefficient of determination, R^2 of 0.9997.

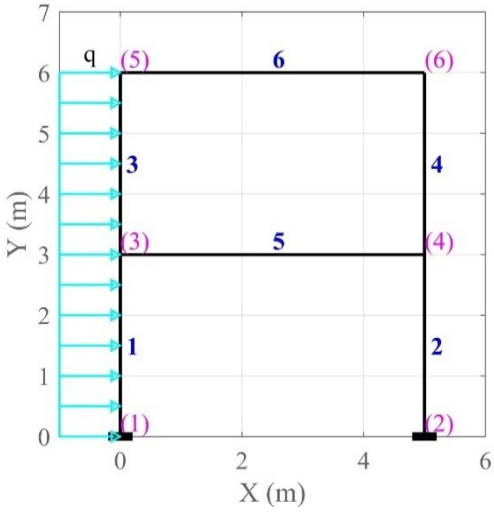

Fig. 6. The two-story frame in Example 2

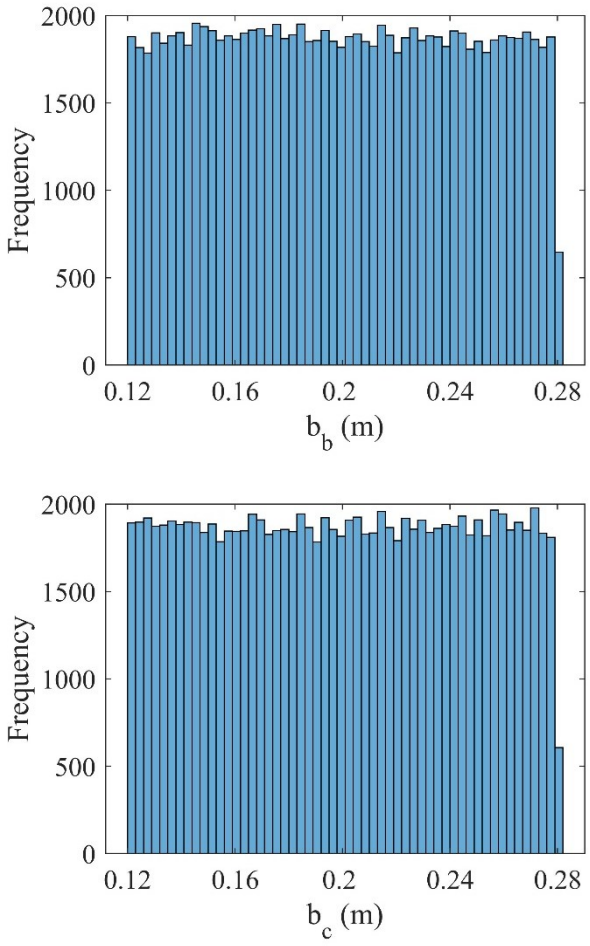

Fig. 7. Simulations of random inputs for Example 2

Table 2. CCD sample sets for the RSFs of Example 2

No	b_b	b_c	b_b^2	b_c^2	$b_b \times b_c$	FS
1	0.1800	0.1800	0.0324	0.0324	0.0324	1.0703
2	0.1800	0.2200	0.0324	0.0484	0.0396	1.2282
3	0.2200	0.1800	0.0484	0.0324	0.0396	1.1326
4	0.2200	0.2200	0.0484	0.0484	0.0484	1.3082
5	0.1717	0.2000	0.0295	0.0400	0.0343	1.1343
6	0.2283	0.2000	0.0521	0.0400	0.0457	1.2353
7	0.2000	0.1717	0.0400	0.0295	0.0343	1.0665
8	0.2000	0.2283	0.0400	0.0521	0.0457	1.3031
9	0.2000	0.2000	0.0400	0.0400	0.0400	1.1893

$$FS = 0.0032 + 1.7928b_b + 4.1746b_c - 5.5444b_b^2 - 5.5155b_c^2 + 11.0347b_b b_c \quad (4)$$

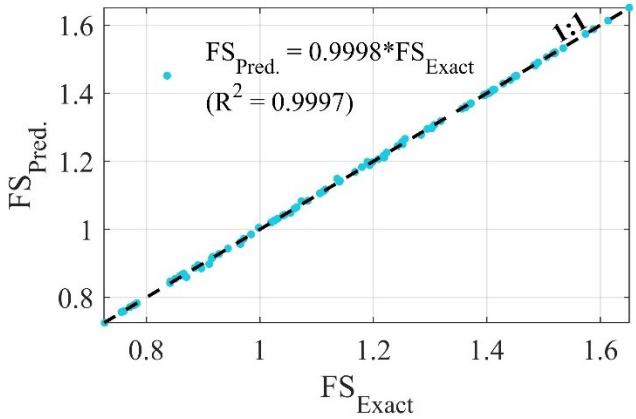

Fig. 8. Validations of RSF in Example 2

Based on the accurate RSF constructed, the proposed optimization procedure is implemented, and the results are presented in Fig. 9. Fig. 9(a) illustrates the estimated drifts for 100,000 samples, where dark markers indicate the cases exceeding the 1.5 cm constraint, while green dots represent feasible samples. Samples with drifts close to the threshold are highlighted by circular markers. It is evident that numerous cases result in threshold drift; however, the corresponding structural weights (depicted by the structure's volume in the vertical axis) vary significantly. Specifically, for the same drift value, the structure's volume can range from 0.82 m³ to 1.29 m³, differing by approximately 1.5 times. Fig. 9(b) summarizes 100 cases at the limit state, with the optimal solution—satisfying the constraint while minimizing the frame's weight—denoted by the star marker. The results indicate that the optimal beam and column widths are 12 cm and 19 cm, respectively.

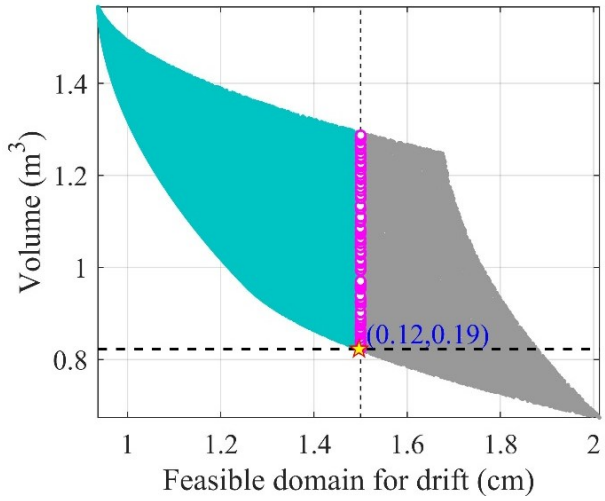

(a)

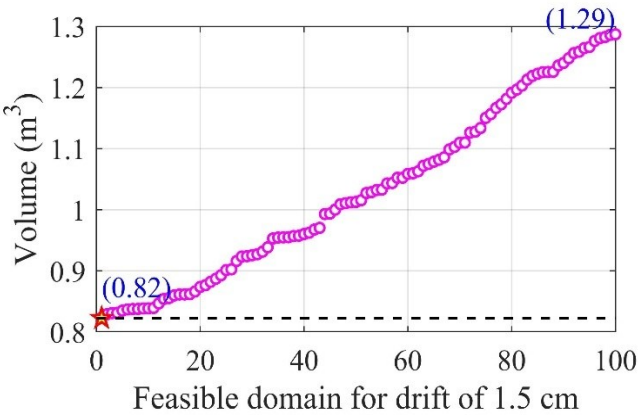

(b)

Fig. 9. Results of Example 2: (a) predicted volumes and drifts for all samples; (b) feasible solutions at the limit state

3.3. Example 3

In this example, a truss structure shown in Fig. 10 is analyzed. The truss consists of 23 members connected at 13 nodes and is subjected to six concentrated loads at the upper nodes. The optimization problem aims to determine the cross-sectional areas of the truss members to minimize

their total weight. The constraints include limiting the maximum deformation to 1/300 of the span length and satisfying the strength requirements of all members. Mathematically, the optimization problem can be formulated by Eq. 5.

$$V_{Opt} = \min V = \arg\min_{A_i}\left(\sum_{i=1}^{23} L_i A_i\right)$$
$$\text{s.t.} \quad FS_{Ser} \geq 1 \qquad (5)$$
$$FS_{Str} \geq 1 \quad (i = 1-23)$$

Here, L and A are the lengths and the cross-sectional areas of the truss elements. FS_{Ser} and FS_{Str} denote the safety factors for serviceability and strength conditions, respectively, as defined in Eq. (6). In Eq. (6), u_i represents the nodal deformations, while P_r and N correspond to the resistance capacities and axial forces in truss bars.

$$FS_{Ser} = \min\left(\frac{L/300}{u_i}\right), \; i = 1-13 \qquad (6a)$$

$$FS_{Str} = \min\left|\frac{P_r}{N_i}\right|, \; i = 1-23 \qquad (6b)$$

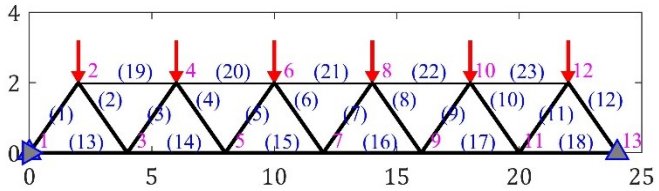

Fig. 10. The truss structure in Example 3

To simplify the problem, the truss members are classified into three groups: lower, upper, and bracing members, with corresponding cross-sectional areas of A_t, A_c, and A_d, respectively. Circular cross-sections are selected for all members, and the design follows AISC 360-16, including checks for buckling in compression members. Further details on truss member design using AISC 360-16 can be found in previous studies, e.g., [25,26].

Using the BBD, the RSM is applied to develop RSFs for predicting FS_{Ser} and FS_{Str}. The accuracy of the RSFs is then validated against the true responses of the truss problem, as shown in Fig. 11 for 100 random samples. The figures show that the RSFs yield responses identical to those of the actual system, as evidenced by R^2 values of unity.

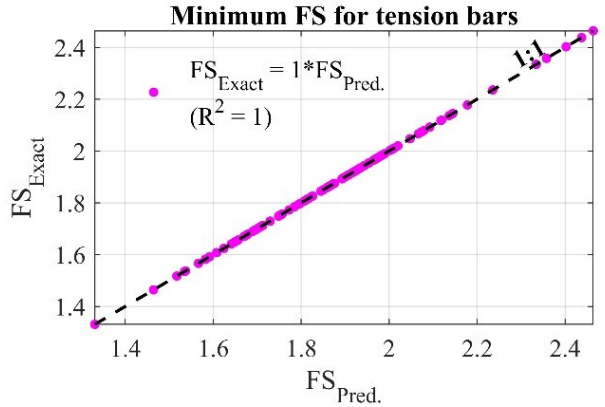

(a)

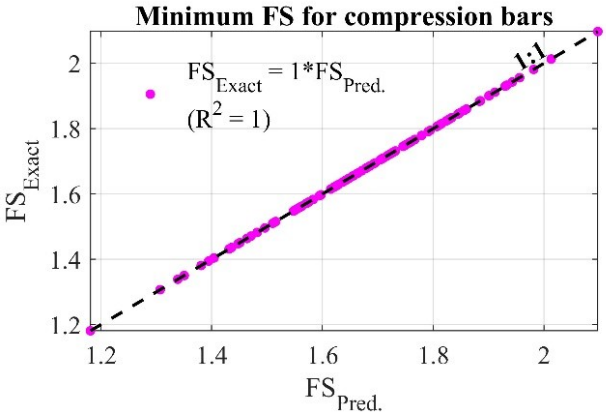

(b)

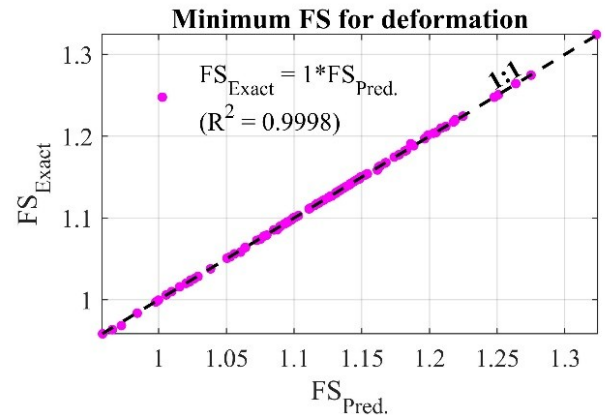

(c)

Fig. 11. Validations of RSFs for truss example: (a) for tension bar; (b) for compression bar; (c) for deformation

The RSFs are then used to predict the responses for 1,000,000 samples in the search for the optimal solution. Fig. 12 illustrates the relationship between safety factors and the volumes of all samples. In the figure, feasible design solutions (i.e., FS≥1) are represented by cyan dots, while approximate limit cases are

marked in red. The optimal solution is highlighted by the black dot. Based on the estimated optimal volume, the cross-sectional areas for lower, upper, and diagonal bars are determined as 4.375, 4.588, and 1.388 cm^2, respectively. The results demonstrate that by leveraging the explicit RSFs, responses can be efficiently obtained even for a large sample set, highlighting the superior performance of the proposed method.

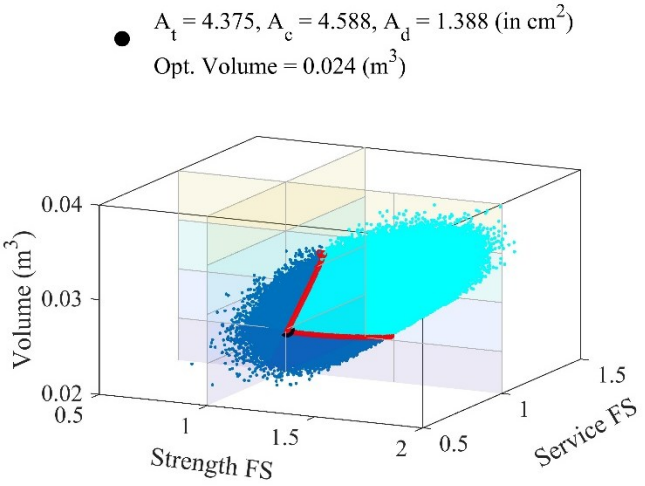

Fig. 12. Predictions for all samples in Example 3

4. Discussions

Based on the three illustrative examples, it is evident that the proposed method can provide accurate solutions. The following subsections thoroughly examine the effectiveness of the proposed procedure.

4.1. Effects of distribution types

Normal and uniform distributions, referred to as ND and UD, respectively, are commonly used in practice for generating random sets of design variables. Fig. 13(a) compares the sample distributions of the section height in Example 1. Notably, a coefficient of variation of 20% is applied to ND, and 1 million samples are generated in Fig. 13(a). The figure shows that while UD produces samples uniformly distributed across the input domain, ND tends to concentrate samples around the mean.

The proposed optimization routine is then applied to predict the responses for the sample set generated by ND, with results presented in Fig. 13(b). It is observed that the best solution from ND-generated samples is suboptimal compared to that from UD, yielding an optimal volume of 0.122 m^3 versus 0.111 m^3 (Figs. 3 and 5). This discrepancy arises because the optimal solution in Example 1 is located at the boundary of the input domain (h = 0.72 m), whereas ND rarely generates samples near the boundaries (Fig. 13(a)). Hence, UD is suggested in the practice.

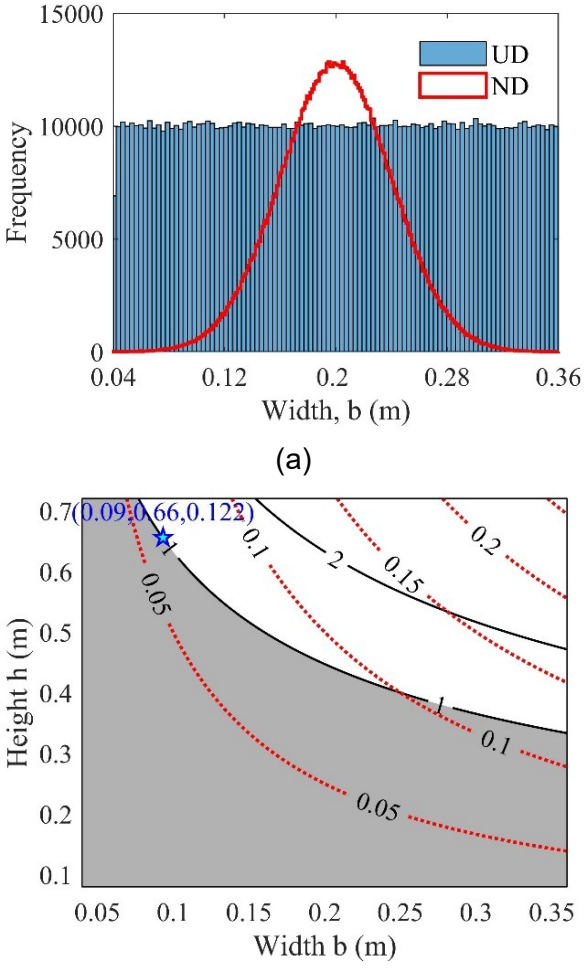

Fig. 13. Effects of distribution types for Example 1: (a) sample sets for section width; (b) solution searched from the normal distributions-based samples

4.2. Effects of formats of RSF

In practice, linear and quadratic polynomials are commonly used to construct RSFs [10,18]. This subsection examines the accuracy of RSFs, considering linear formulations as well as full and reduced quadratic polynomials.

Fig. 14 compares 1,000 safety factors predicted by three RSF models (FS^{RSM}) – linear

($FS^{(l)}$), reduced quadratic ($FS^{(2,r)}$), and full quadratic ($FS^{(2,f)}$) – against the true values (FS^{FEM}) for Example 2. The accuracy of the models is evaluated using the coefficient of determination (R^2) reported in the figure. The results show that the full quadratic polynomial provides the most accurate estimations, as evidenced by an R^2 value of 0.9997. Based on this analysis, the full quadratic polynomial model is recommended for structural response predictions.

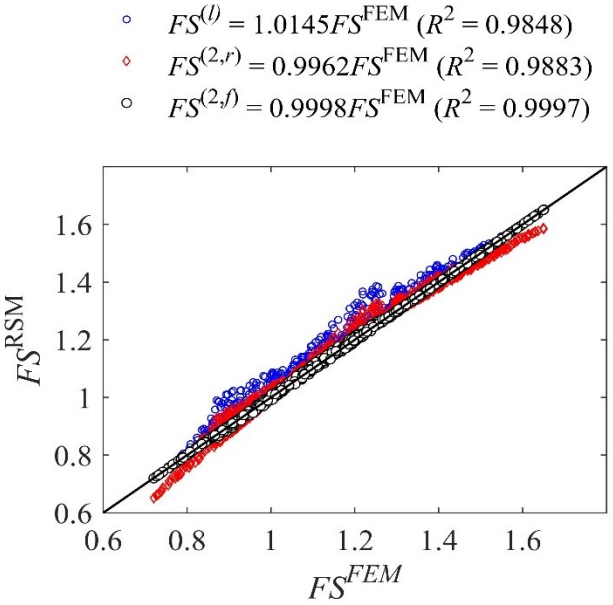

Fig. 14. Effects of RSFs for Example 1

4.3. Evaluations on sample size and computing time

The computational time for optimization problems is affected by the size of the sample set, especially when constraints are defined implicitly, such as safety factors in Examples 2 and 3. This section examines the impact of sample size on computational time in the proposed procedure for Example 3.

To assess the impact of sample size on the optimization procedure, ten different sample sizes ranging from 100,000 to 1 million are considered, and the corresponding optimal volumes are summarized in Fig. 15. The computational time (in milliseconds, (using a Dell laptop with 16 GB RAM and one Intel Core i7 CPU @ 3.0 GHz)) required for predicting and identifying the optimal solution is also indicated by blue text in the figure. Notably, Example 3 is completed within two seconds, even for the largest sample size of 1 million. Interestingly, the computation time increases by only about a factor of two, even when the sample size increases tenfold, thanks to the exclusive use of explicit functions in the proposed procedure. In general, larger sample sizes result in smaller optimized volumes. However, the variation in optimal volume remains minor across the ten sample sizes examined.

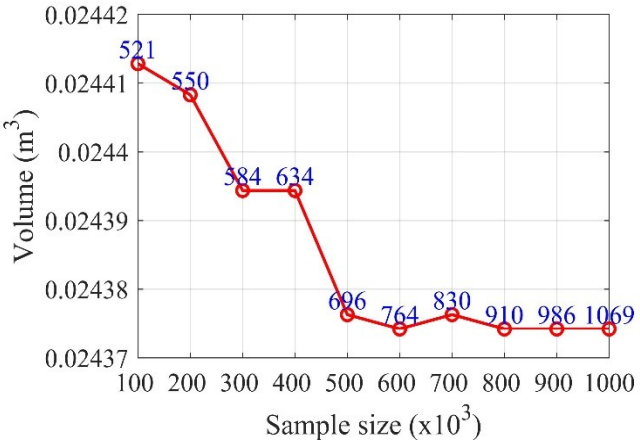

Fig. 15. Effects of sample sizes on Example 3

5. Conclusion

In this study, a computationally efficient procedure is proposed to address the high computational cost of structural optimization. The response surface method is employed to develop explicit functions that approximate the original implicit constraints. A random sampling strategy is utilized to represent the input domains, and the response surface functions are then used to formulate the optimization problem explicitly. This allows the optimal solution to be efficiently identified within the feasible design space.

The accuracy of the proposed RSM-based optimization is validated against analytical solutions in Example 1, demonstrating its reliability. Across three examples, high coefficients of determination confirm the precision of the RSM in approximating computational evaluations of structural problems. Among the investigated models, the full quadratic polynomial consistently provides the best approximation and is recommended for practical applications.

Furthermore, the study reveals that uniform sampling yields superior optimization results compared to normal sampling. This is because the uniform distribution ensures better coverage of the design space, making it particularly effective when the optimal solution lies near the domain boundaries.

A key advantage of the proposed procedure is its computational efficiency. Even when evaluating up to a million samples, the optimization process is completed in just seconds. This highlights the robustness and practicality of the method for handling complex structural optimization problems, making it a valuable tool for engineering applications.

References

[1] O.C. Zienkiewicz, R.L. Taylor. (2005). The finite element method set (Vols. 1-3). *Butterworth-Heinemann*.

[2] R.D. Cook, D.S. Malkus, M.E. Plesha, R.J. Witt. (2002). Concepts and Applications of Finite Element Analysis. 4th edition. *Willey*.

[3] D.L. Logan. (2010). A first course in the finite element method. 5th ed. *CL Engineering*.

[4] A.K. Chopra. (2012). Dynamics of Structures Theory and Applications to Earthquake Engineering. 4th ed. *Prentice Hall. Pearson*.

[5] T. Belytschko, W.K. Liu, B. Moran, K.I. Elkhodary. (2014). Nonlinear Finite Elements for Continua and Structures. vol. 38. 2nd ed. *Wiley*.

[6] C.-T. Nguyen, H.-Q. Chu, T.-S. Vu, X.-T. Le, C.-T. Dinh. (2023). Numerical analysis of aerodynamic and structure characteristics of an autonomous unmanned flying car for high-rise building rescue operations in urban area. *Journal of Science and Transport Technology*, 3(4), 1-9.

[7] D.V. Hung, N.T. Phu. (2023). Towards a generalized surrogate model for truss structure analysis using graph learning. *Journal of Science and Technology in Civil Engineering - HUCE*, 17(2), 99-109.

[8] K.J. Bathe. (1996). Finite Element Procedures. *Prentice Hall*.

[9] H.-B. Dinh, V.H. Mac, N.S. Doan. (2024). Comparative study on semi-probabilistic design methods to calibrate load and resistance factors for sliding stability design of caisson breakwaters. *Ocean Engineering*, 293, 116573.

[10] N.S. Doan, V.H. Mac, H.-B. Dinh. (2024). Efficient optimization-based method for simultaneous calibration of load and resistance factors considering multiple target reliability indices. *Probabilistic Engineering Mechanics*, 78, 103695.

[11] J. Huh. (2000). Reliability analysis of nonlinear structural systems using response surface method. *KSCE Journal of Civil Engineering*, 4(3), 135-143.

[12] N.S. Doan, H.-B. Dinh. (2024). Effects of limit state data on constructing accurate surrogate models for structural reliability analyses. *Probabilistic Engineering Mechanics*, 76, 103595.

[13] P. Chen, C. Zhao, H. Yao, J. Li. (2023). System reliability analysis for truss structures based on automatic updated model. C - *Computer Modeling in Engineering & Sciences*, 134(3), 2057-2071.

[14] T.-A. Nguyen, H.-B. Ly. (2021). Estimation of the bond strength between FRP and concrete using ANFIS and hybridized ANFIS machine learning models. *Journal of Science and Transport Technology*, 1(1), 34-44.

[15] S. Chai, X.-F. Ji, L.J. Li, M. Guo. (2018). Multivariate rational response surface approximation of nodal Displacements of truss structures. *Chinese Journal of Mechanical Engineering*, 31, 1.

[16] R.A.S. Díaz, S.J.S. Nova, M.C.A. Teixeira da Silva, L.M. Trautwein, L.C. de Almeida. (2020). Reliability analysis of shear strength of reinforced concrete deep beams using NLFEA. *Engineering Structures*, 203, 109760.

[17] K. Winkelmann. (2018). Probabilistic methods in reliability assessment of engineering lightweight structures. *XXIV Lightweight Structures in Civil Engineering*

Contemporary Problems, 147-157.

[18] R.H. Myers, D.C. Montgomery, C.M. Anderson-Cook. (2009). Response surface methodology. 3rd ed. *Wiley*.

[19] V.-H. Truong, H.M. Hung, P.H. Anh, T.D. Hoc. (2020). Optimization of steel moment frames with panel-zone design using an adaptive differential evolution. *Journal of Science and Technology in Civil Engineering - HUCE*, 14(2), 65-75.

[20] H.D. Phan, S.V. Phan. (2024). Cost optimization in structural design for reinforced concrete frames using Jaya algorithm. *Journal of Science and Technology in Civil Engineering - HUCE*, 18(3), 76-91.

[21] R. Yang, W. Li, Y. Liu. (2022). A novel response surface method for structural reliability. *AIP Advances*, 12(1), 015205.

[22] J. Ji, B.K. Low. (2012). Stratified Response Surfaces for System Probabilistic Evaluation of Slopes. *Journal of Geotechnical and Geoenvironmental Engineering*, 138(11), 1398-1406.

[23] J. Huh, A. Haldar. (2001). Stochastic Finite-Element-Based Seismic Risk of Nonlinear Structures. *Journal of Structural Engineering*, 127(3), 323-329.

[24] S.H. Lee, B.M. Kwak. (2006). Response surface augmented moment method for efficient reliability analysis. *Structural Safety*, 28(3), 261-272.

[25] N.S. Doan, A.T. Tran. (2025). Comparative Study on the Probabilistic Safety of Truss Structures Designed Using U.S. and Vietnamese Codes. *Journal of Science and Transport Technology*, 5(1), 1-14.

[26] S.N. Doan. (2024). Probabilistic safety assessments of truss structures designed by AISC 360-16 and EC 3. *Journal of Science and Technology in Civil Engineering - HUCE*, 18(2), 149-162.